



All-optical switching of magnetization in atomically thin CrI₃

Peiyao Zhang¹, Ting-Fung Chung¹, Quanwei Li¹, Siqi Wang¹, Qingjun Wang^{2,3}, Warren L. B. Huey⁴, Sui Yang^{1,5}, Joshua E. Goldberger⁴, Jie Yao^{1,6} and Xiang Zhang^{1,6}  

Control of magnetism has attracted interest in achieving low-power and high-speed applications such as magnetic data storage and spintronic devices. Two-dimensional magnets allow for control of magnetic properties using the electric field, electrostatic doping and strain. In two-dimensional atomically thin magnets, a non-volatile all-optical method would offer the distinct advantage of switching magnetic states without application of an external field. Here, we demonstrate such all-optical magnetization switching in the atomically thin ferromagnetic semiconductor, CrI₃, triggered by circularly polarized light pulses. The magnetization switching behaviour strongly depends on the exciting photon energy and polarization, in correspondence with excitonic transitions in CrI₃, indicating that the switching process is related to spin angular momentum transfer from photoexcited carriers to local magnetic moments. Such an all-optical magnetization switching should allow for further exploration of magneto-optical interactions and open up applications in high-speed and low-power spintronic devices.

On-demand magnetic responses to external stimuli are at the heart of modern magnetism and enable applications such as magnetic memory, data storage and spintronic devices. In recently discovered two-dimensional (2D) van der Waals layered magnets, such as CrI₃ (ref. ¹) and CrGeTe₃ (ref. ²), controlling magnetic properties including magnetic states and magnetic phase transitions has been demonstrated using various methods including electrostatic doping, applying electric field, strain and so on^{3–11}. The control of magnetic states using the electrical methods requires continuous application of the external magnetic field, since the magnetic states sensitive to electrostatic doping and electric fields are close to the metamagnetic transitions at the coercive field^{3,4}. A non-volatile method that can control the magnetic states without the application of an external magnetic field is critically needed and would benefit both fundamental physics studies and device applications¹².

Photons have been used to deterministically control magnetism through the interplay between circularly polarized light pulses and magnetic moments¹³. This is referred to as helicity-dependent all-optical switching and has enabled the development of ultrafast magneto-optical memory devices, such as all-optical magnetic recorders. Compared to other methods, all-optical control of magnetism does not require an external magnetic field and has the potential to increase the magnetic reversal speed into terahertz frequencies¹³. Previous studies have demonstrated the optical control of magnetization on various metallic ferrimagnetic and ferromagnetic rare-earth transition-metal thin films^{13–15}, such as GdFeCo alloys and Co/Pt multilayers. However, the metallic magnetic thin films in which all-optical switching has been achieved cannot offer the electrical modulation functionalities that have been exhibited in semiconductors, which limits their potential application in spintronics devices. In addition, the microscopic origin of the all-optical switching observed in the above-mentioned systems is still under debate^{16,17}. The observed all-optical magnetization switching was

first explained using the inverse Faraday effect (IFE), where the circularly polarized photons can induce an effective magnetic field to reverse the magnetization^{18,19}. It was later shown that the helicity-dependent absorption in different domains associated with magnetic circular dichroism (MCD) has contributed to the switching of magnetization²⁰. Recent works have suggested that magnetization switching could be achieved by optical spin transfer²¹ and strong coupling between photoexcited carriers and lattice magnetic moments²². Here in ferromagnetic CrI₃, the semiconducting nature offers a platform to study the all-optical switching of magnetization when addressing different excitonic transitions and to investigate the interplay among light, excitons and magnetism.

A previous study has shown that in (Ga, Mn)As, ferromagnetic semiconductors, optically excited carrier spins will create a photo-induced magnetization that largely changes the net total magnetization in the material, but does not flip the spin state entirely²³. The all-optical switching of magnetization has not been realized in ferromagnetic semiconductors, to the best of our knowledge. Recently discovered atomically thin ferromagnetic semiconductors, such as CrI₃, feature out-of-plane magnetizations¹ and exhibit strong optical absorptions²⁴ and giant excitonic and magneto-optical responses^{22,25}, making them attractive candidates for this effect. Utilizing the above-mentioned characteristics in CrI₃, we demonstrate an all-optical approach to deterministically switch magnetization in CrI₃ by exciting with circularly polarized photons. Due to the semiconducting nature, by varying the exciting photon energy, we are able to address different excitonic transitions and study how excited carriers at different orbitals affect the all-optical switching behaviour. Our results show that the magnetization switching depends strongly on the exciting photon energy and polarization, as schematically illustrated in Fig. 1a. Circularly polarized pulse lasers with opposite circular polarizations can be used to switch the magnetization of CrI₃ from the up to the down state at different excitation energies. The strong energy and polarization-dependent

¹Nano-scale Science and Engineering Center (NSEC), University of California, Berkeley, CA, USA. ²Department of Materials Science and Engineering, University of California, Berkeley, CA, USA. ³Materials Sciences Division, Lawrence Berkeley National Laboratory, Berkeley, CA, USA. ⁴Department of Chemistry and Biochemistry, The Ohio State University, Columbus, OH, USA. ⁵School for Engineering of Matter, Transport and Energy, Arizona State University, Tempe, AZ, USA. ⁶Faculty of Science and Faculty of Engineering, The University of Hong Kong, Hong Kong, China.  e-mail: xiang@berkeley.edu

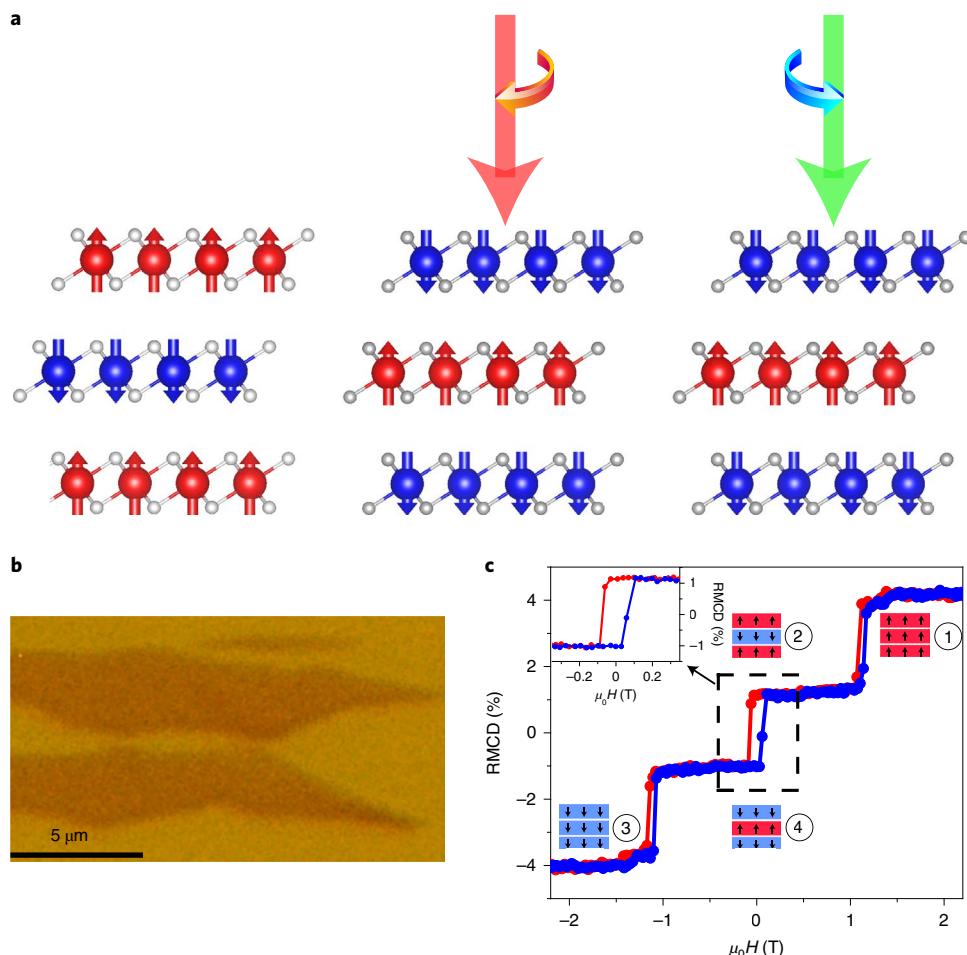


Fig. 1 | All-optical magnetization switching in atomically thin magnetic crystal of CrI_3 and sample characterization. **a**, Schematic representation of the all-optical magnetization switching in three-atomic-layer-thin CrI_3 (a layered antiferromagnetic semiconductor) with circularly polarized pulsed irradiations with different photon energies. The left panel shows the spin configuration of 3L CrI_3 magnetized in the upward direction without an applied magnetic field. The middle (right) panel shows the circularly polarized pulsed laser illumination with excitation energy between 1.7 and 2.1 eV (above 2.1 eV) that is used to switch the magnetization from the up to the down state. The switching of the magnetization from the up to the down state was achieved by using light with different circular polarizations for laser energies between 1.7 and 2.1 eV and above 2.1 eV. **b**, Microscope image of two 3L CrI_3 flakes. **c**, RMCD as a function of applied magnetic field on the top 3L CrI_3 flake, red (blue) data points denote the RMCD value while the magnetic field is sweeping to the negative (positive) direction. Magnetic states (1–4) at different applied fields are shown as schematic diagrams in the insets. Red (blue) colour in the magnetization state schematic diagrams represents that the entire CrI_3 layer is magnetized in the upward (downward) direction. In the experiment, the magnetic field is withdrawn from positive (negative) fields to magnetize the entire flake to state 2 (4), and a pulsed laser is applied at zero applied field to achieve the all-optical magnetization switching. The upper inset shows a zoomed view of the curves in the black dashed box.

magnetization switching behaviours indicate that the magnetization switching is related to spin angular momentum transfer between excited carriers and localized magnetic moments. This all-optical approach of magnetization control offers the basis for future ultrafast all-optical magnetic memory and logic processing devices based on 2D magnets, as well as for future theoretical and experimental investigations of the microscopic mechanisms of the observed physical phenomenon.

We prepared trilayer (3L) CrI_3 flakes by mechanically exfoliating bulk CrI_3 crystal onto 300 nm SiO_2/Si substrates and encapsulating with hexagonal boron nitride (hBN) in a N_2 glove box to prevent sample degradation. An optical microscopy image of two 3L CrI_3 flakes used in this study is shown in Fig. 1b. We utilized reflectance magneto-circular dichroism (RMCD) images (shown in Fig. 2a–d) to measure the out-of-plane magnetization before and after the illumination of the circularly polarized laser pulses. A 633 nm He–Ne laser with $\sim 1 \mu\text{m}$ beam spot and $\sim 5 \mu\text{W}$ optical power was used for all RMCD measurements unless otherwise stated. To study

the all-optical magnetization switching, a second ultrafast laser with ~ 100 fs pulse duration was used to excite the samples. RMCD images were recorded before and after the pulsed laser (either circularly or linearly polarized) swept through the entire or partial area of the sample to study the initial magnetization state and the magneto-optical response to the polarized laser pulses. All the measurements were performed at 1.6 K unless otherwise stated.

A representative RMCD signal as a function of an applied out-of-plane magnetic field is shown in Fig. 1c. The red (blue) curve represents the RMCD signal when the magnetic field is swept from a positive (negative) to a negative (positive) direction. For the absolute value of the applied magnetic field $|\mu_0 H| > 1.1$ T, the magnetization of all three layers of CrI_3 align in the same direction (upward or downward depending on the field direction) as depicted in the magnetization configuration schematics (magnetic states 1 and 3). When the magnetic field is withdrawn to zero, due to the interlayer antiferromagnetic coupling¹, the 3L CrI_3 possesses a non-zero remnant magnetization, which is solely determined by the spins

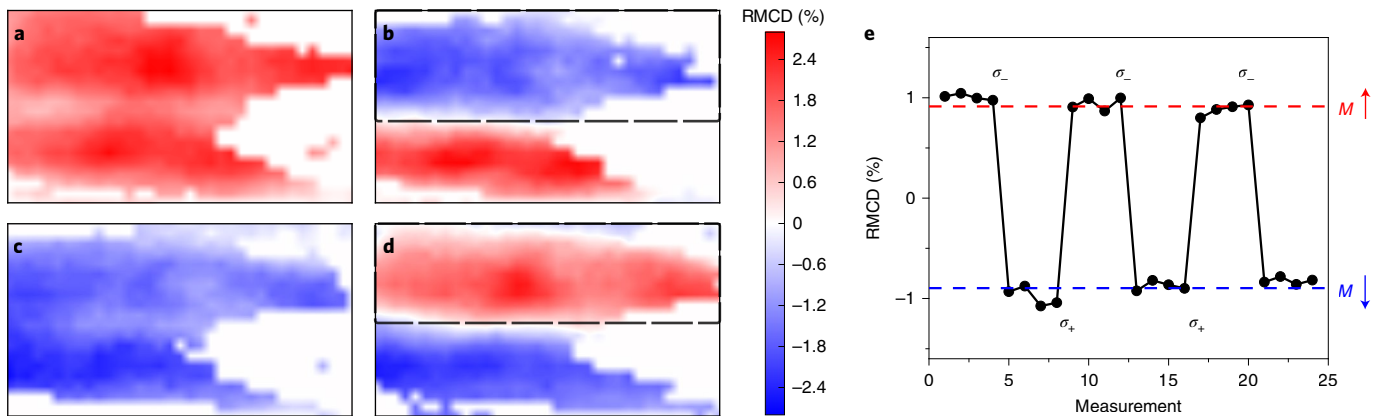


Fig. 2 | Experimental demonstration of all-optical magnetization switching in 2D CrI₃. **a-d**, Spatial RMCD maps at zero applied magnetic field, withdrawn from +2 T (**a** and **b**) and -2 T (**c** and **d**). The spatial RMCD maps are acquired before (**a** and **c**) and after (**b** and **d**) circularly polarized pulsed light exposure at 2.03 eV in selected areas (indicated by the dashed box). As shown in the figures, the deterministic magnetization in selected CrI₃ flakes is achieved by circularly polarized pulsed laser illumination regardless of the initial magnetization state of the material. The deterministic magnetization switching can be achieved in a selected sample area without application of an external magnetic field. **e**, Repeated deterministic switching measurements between states 2 and 4 by circularly polarized pulsed irradiation at 2.03 eV, red (blue) dashed line indicates the magnetic state 2 (4) in Fig. 1c and *M* stands for the net magnetization of the flake. Without the application of an external magnetic field, the magnetization states can be deterministically switched by the circularly polarized photons.

of the unbalanced layer. Thus, at zero field, the net magnetization of the 3 L CrI₃ has a magnetic memory and an orientation that we define as upward in state 2 and downward in state 4, if the field was ramped to zero from a positive and negative direction, respectively. In all-optical magnetization switching experiments, the magnetic field is swept to zero from either a positive or negative direction to initialize the magnetization state of the 3 L CrI₃ before the illumination of the pulsed laser. All the RMCD mapping measurements were carried out at zero applied magnetic field.

With the magnetization set to be either a positive (state 2) or negative (state 4) direction, we are able to study how the 3 L CrI₃ responds to the circularly polarized photon pulses. Figure 2a,c shows the RMCD images of the two 3 L CrI₃ flakes at zero field swept from positive and negative 2 T, respectively. Red and blue colours represent the net out-of-plane magnetization being in the upward and downward directions, respectively. The effect of polarized laser pulses on CrI₃ magnetization is demonstrated by sweeping the circularly polarized 2.03 eV photon pulses selectively on the top flake indicated by the dashed box in Fig. 2b,d. Remarkably, as illustrated in the figures, the magnetization of the regions illuminated with circularly polarized photons turns into an upward or a downward direction depending only on the helicity of the photons. Specifically, with a photon energy of 2.03 eV, right circularly polarized (RCP) (σ_-) will switch the CrI₃ magnetization to a down state, and left circularly polarized (LCP) light (σ_+) will switch the CrI₃ magnetization to an up state regardless of the initial magnetization state. By stark contrast, when both flakes are exposed to linearly polarized photons, multiple domains with random magnetization directions appear on the flakes as shown in Supplementary Fig. 1. The large domain size and small number of domains indicate that the domain wall formation energy is large relative to the magneto-static energy in CrI₃ flakes compared to in magnetic thin films such as GdFeCo and Co/Pt multilayers, where many small domains with random orientations are formed after linearly polarized light illumination^{13,14,26}. Supplementary Fig. 2 summarizes the magnetization switching of CrI₃ using 2.03 eV circularly polarized light pulses with various laser fluences. It is shown that, with the highest power available, no thermal demagnetization is observed, which indicates that the temperature of the sample did not exceed the Curie temperature T_c of CrI₃ within the laser pulse duration. This is very different from the metallic Co/Pt multilayer, in which twice the deterministic

switching power is enough to realize the thermal demagnetization¹⁴. This result shows low laser-induced lattice heating in the ferromagnetic semiconductor and hints that the thermal contribution from the exciting laser is not the main factor responsible for the switching of magnetization in CrI₃. In Fig. 2e we demonstrate the deterministic magnetization state switching utilizing circularly polarized pulsed photons by performing four consecutive RMCD measurements at a fixed spot on the sample between two circularly polarized pulsed laser scans. The selective (Supplementary Fig. 3) and deterministic control of magnetization has the potential to achieve 2D magnet-based magnetic storage and processing applications.

Unlike in the metallic ferrimagnetic thin film systems in which varying the excitation photon energy does not affect the power threshold for all-optical magnetization switching²⁷, the semiconducting nature of CrI₃ offers a platform to control the magnetization switching processes using different optical excitations. Here, we first magnetize the entire flakes to an up state by sweeping the magnetic field to zero from the positive side. After scanning the entire flake using laser pulses with fixed polarization (RCP, σ_-) and various photon energies and pulse fluences, we record the final magnetization state of the flake and summarize the switching threshold in Fig. 3a. In this figure, the solid and half-filled triangles represent the laser fluence of the photon energy that is sufficient to either fully or partially (Supplementary Fig. 4) switch the magnetization of the flake, respectively, while the crosses correspond to the excitation energies in which the magnetization remains unchanged after polarized light exposure. The red and blue colours map out regions, showing whether deterministic switching was achieved. Surprisingly, when using σ_- polarized light, the switching fluence has a strong dependence on the exciting photon energy. Even with the highest power available, σ_- polarized light with photon energies above 2.1 eV and below 1.7 eV cannot disturb the magnetization state of the flake. By contrast, with a photon energy between 1.7 eV and 2.1 eV, the polarized photons can effectively switch the magnetization state of the sample, and the power threshold lowers dramatically when approaching 1.9 eV from both directions.

To further investigate the all-optical switching behaviour in CrI₃, we performed a similar study using left circularly polarized (σ_+) light, and the results are shown in Fig. 3b. As shown in the figure, for photon energies above 2.1 eV, the magnetization transition from the up to down state can be realized using LCP light. The down to up magnetization

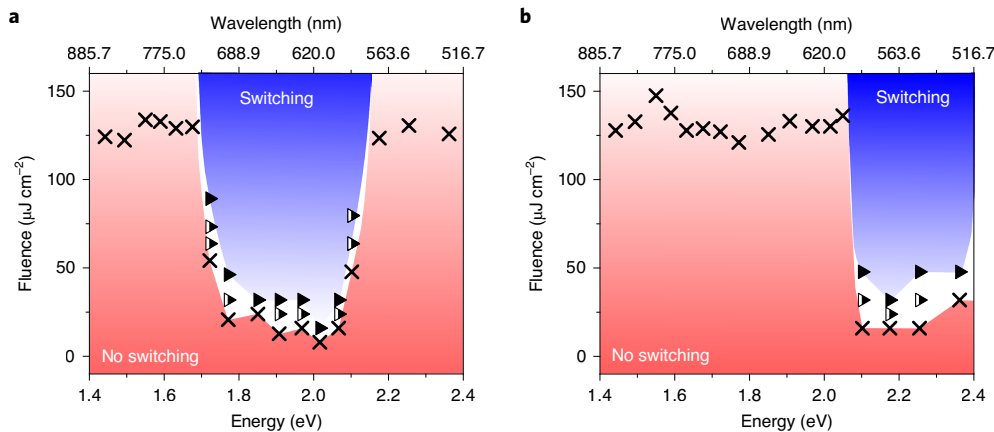


Fig. 3 | Fluence-dependent magnetization switching phase diagram for circularly polarized exciting photons with different energies. **a,b**, Fluence threshold phase diagram of all-optical magnetization switching from the up to the down state in 3L CrI₃ using σ_- (**a**) and σ_+ (**b**) circularly polarized pulsed photons. Solid and partially filled triangles represent the magnetization of the flake being fully or partially switched, respectively, using the selected laser fluence at different excitation energies, while crosses represent no magnetization switching being achieved. Three energy regions with switching behaviours are shown: (1) For energies below 1.7 eV, magnetization cannot be switched by circularly polarized light; (2) for energies between 1.7 and 2.1 eV, up-to-down-state magnetization switching is achieved by excitation with σ_- photons; and (3) for energies above 2.1 eV, magnetization is flipped from an up to a down state with σ_+ photon excitation. This energy-dependent and polarization-dependent magnetization switching behaviour was not observed in the previously studied systems and strongly relates to the various excitonic transitions in semiconducting CrI₃.

switching is achieved using RCP light with photon energies above 2.1 eV (Supplementary Fig. 5). We have studied both 3L and 5L CrI₃ samples. All show similar magnetization switching behaviours. (Supplementary Figs. 6 and 7). To better understand the switching behaviour for exciting photons with different energies, we performed broadband white light absorption measurements on a CrI₃ flake with the same thickness deposited on a sapphire substrate. The measured differential reflectance spectrum is proportional to the absorption spectrum^{24,28,29}. Four prominent absorption features labelled as i, ii, iii and iv and centred around 1.7, 1.9, 2.4 and 2.6 eV are shown in Fig. 4a. The energies of features ii, iii and iv (but not i) are very similar to previously reported results^{24,25,30}. This is due to the low quantum yield efficiency of the detector used in this study at energies below 1.7 eV; it cannot detect the entire feature of the lowest energy transition. The transition energy for feature i is at around 1.5 eV, as shown in the previous studies^{24,25}. The energy regions for different magnetization switching behaviours (Fig. 3) match very well with the observed absorption transitions. When the photon energy excites the Cr *d*-*d* transitions centred at 1.5 eV, the circularly polarized light cannot flip the magnetization state in CrI₃. When the incident photon pulses acquire an energy large enough to excite the ligand-to-metal transitions at around 1.9 eV and 2.3 eV, RCP and LCP light, respectively, with sufficient power can trigger an up-to-down state magnetization switching. This indicates that the all-optical magnetization switching in CrI₃ has a strong connection to the specific excited electronic transitions and to the angular momentum transfer between the excited carrier spins and the spins of the valence electrons, which predominantly contribute to the out-of-plane magnetization.

To better understand the underlying mechanism in all-optical control of magnetism in CrI₃, we first review the IFE^{19,31} and MCD^{20,27} mechanisms, which mainly contribute to the previously observed all-optical helicity-dependent magnetization switching in ferrimagnetic and ferromagnetic thin films. In the IFE mechanism, an alternating electric field in circularly polarized light leads to circular electron motion in a material, which will induce an effective magnetic field and affect the magnetization^{19,31}. However, the direction of the induced magnetic field is solely dependent on the optical circular polarization regardless of the photon energy. Here in CrI₃, it is clearly shown in Fig. 3a,b that opposite circular polarized photons with different energies (above and below 2.1 eV) have the

same effect in changing the magnetic state, thus ruling out IFE as the dominant factor in magnetization switching in CrI₃. The MCD mechanism proposes that the thermal energy provided by the first circularly polarized laser pulse will cause the temperature difference among regions with different magnetizations due to MCD. At the appropriate laser fluence, the temperature of the hotter regions is slightly higher than the Curie temperature T_c , while the cooler regions still have a temperature below T_c . After the first laser pulse, the temperature will relax back to below T_c and the hotter region will experience a paramagnetic to ferromagnetic phase transition and have an even distribution of magnetic domains with upward and downward magnetizations as a result. Thus, multiple light pulse exposures will result in a favourable magnetic state that absorbs less with regard to certain circularly polarized photons²⁰. To evaluate the thermal contribution of the exciting laser pulses in CrI₃ magnetization switching, we performed the MCD measurements as a function of applied magnetic field with three different laser excitations: 1.58, 1.96 and 2.33 eV. As shown in Fig. 4c,d, when the field is withdrawn to zero from the positive direction (red curve), the MCD (defined as $(A_- - A_+)/ (A_- + A_+)$, where A_- (A_+) is the absorption of σ_- (σ_+) polarized photons) is positive when exciting with 1.96 eV photons and negative when exciting with 2.33 eV photons. This shows that the σ_- and σ_+ circularly polarized absorption is dominant for 1.96 and 2.33 eV photons, respectively, and is consistent with observed switching behaviours and a previous theoretical study²⁵. The MCD at zero field is only a few (few tenths of a) percent when using 1.96 (2.33) eV photons. This indicates that the absorption of two types of circularly polarized photons at the same energy is very similar. If the MCD mechanism is valid, one would expect that after reaching the magnetization switching fluence threshold, further increasing fluence would lead to a thermal demagnetization, since regions with both magnetizations would have a temperature higher than T_c after laser pulse exposure given that the absorption difference between different regions with opposite magnetizations for the same type of circularly polarized photons is merely ~1.5% for 1.96 eV (~0.15% for 2.33 eV) photons. However, as shown in Supplementary Fig. 2, a laser fluence of ten times the threshold at 2.03 eV leads to full magnetization switching instead of thermal demagnetization. This clearly excludes MCD from being the mechanism responsible for the observed optical control of magnetization in CrI₃.

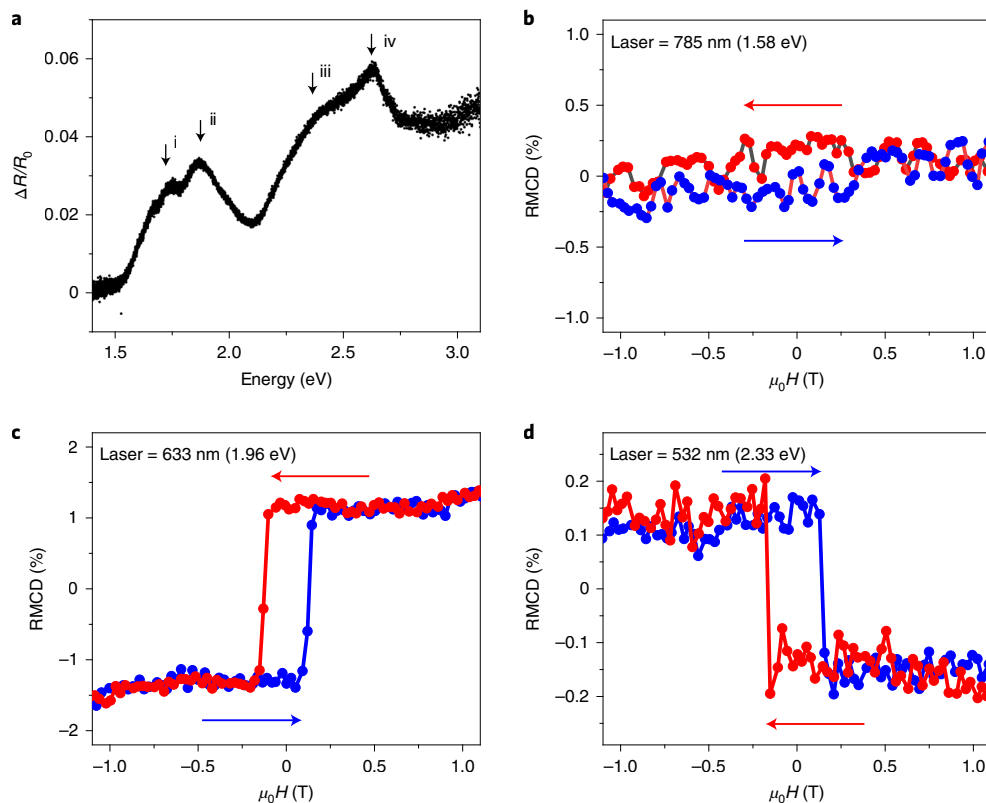


Fig. 4 | Excitonic transitions in 3L CrI₃ and circularly polarized photon absorption difference at selected energies. **a**, Differential reflectance spectrum of 3L CrI₃ on sapphire substrate. Four absorption features in the spectrum are attributed to an internal Cr *d*-*d* orbital transition (feature i) and ligand-to-metal transitions (features ii, iii and iv). The energies for absorption transition features i, ii and iii match very well with the energy regions of different magnetization switching behaviours, suggesting that the magnetization switching is related to the exciton spins at different excitonic transitions. **b-d**, RMCD as a function of applied magnetic field using 1.58 eV **(b)**, 1.96 eV **(c)** and 2.33 eV **(d)** photons measured at 1.6 K, red and blue arrows represent the magnetic field sweeping directions. When the magnetic field is swept to zero from the positive direction, the RMCD signal is positive (negative) when exciting with 1.96 (2.33) eV photons, indicating that the absorption of σ_- (σ_+) polarized photons is dominant for 1.96 (2.33) eV photons. The absorption differences for circularly polarized photons at each excitonic transition align very well with the energy regions in the magnetization switching phase diagram, strongly suggesting the connection between excited carrier spins and the flipping of the magnetic moment.

We propose that the all-optical magnetization switching in CrI₃ is achieved through angular momentum transfer from the photo-excited carrier spins to the spins of the valence electrons occupying the *t*_{2g} orbitals of Cr atoms, instead of the purely thermal process of the MCD mechanism^{21,22,32}. The circularly polarized light will excite electron–hole pairs with a preferred spin direction. The excitons will recombine after relaxing to the valence band maximum and conduction band minimum. The spin angular momentum is transferred from the excited carriers to the valence electrons, from which the magnetization switching is achieved. From the switching behaviours illustrated in Fig. 3a,b, RCP photons with energy between 1.7 and 2.1 eV and LCP photons with energy beyond 2.1 eV lead to the same magnetization state, indicating that photoexcited carriers by two different photons (different regarding both energy and circular polarization) have the same type of spin. This is supported by the opposite trend in the RMCD versus $\mu_0 H$ plots using 1.96 and 2.33 eV lasers as shown in Fig. 4c,d. The absorption imbalance at zero field is caused by the spontaneous splitting between the two states with different spin angular momentum values. The energy of the state with up (down) spin will shift upward (downward) when the magnetization is aligned in the upward direction.

In summary, we have demonstrated selective and deterministic magnetization switching in CrI₃, utilizing a circularly polarized pulsed laser. The unexpected energy-dependent and polarization-dependent switching threshold behaviour points out

the spin angular momentum transfer switching mechanism. Our research provides a better understanding of the interactions between polarized photons and magnetic materials in an all-optical magnetization switching mechanism that is not accessible in other magnetic thin film systems. Our work shows that layered van der Waals ferromagnets present a new platform for exploring all-optical magnetization switching and the potential applications in magneto-optical memory, data storage and processing applications.

Online content

Any methods, additional references, Nature Research reporting summaries, source data, extended data, supplementary information, acknowledgements, peer review information; details of author contributions and competing interests; and statements of data and code availability are available at <https://doi.org/10.1038/s41563-022-01354-7>.

Received: 25 March 2022; Accepted: 4 August 2022;
Published online: 15 September 2022

References

1. Huang, B. et al. Layer-dependent ferromagnetism in a van der Waals crystal down to the monolayer limit. *Nature* **546**, 270–273 (2017).
2. Gong, C. et al. Discovery of intrinsic ferromagnetism in two-dimensional van der Waals crystals. *Nature* **546**, 265–269 (2017).

3. Huang, B. et al. Electrical control of 2D magnetism in bilayer CrI₃. *Nat. Nanotechnol.* **13**, 544–548 (2018).
4. Jiang, S., Li, L., Wang, Z., Mak, K. F. & Shan, J. Controlling magnetism in 2D CrI₃ by electrostatic doping. *Nat. Nanotechnol.* **13**, 549–553 (2018).
5. Cenker, J. et al. Reversible strain-induced magnetic phase transition in a van der Waals magnet. *Nat. Nanotechnol.* **17**, 256–261 (2022).
6. Jiang, S., Xie, H., Shan, J. & Mak, K. F. Exchange magnetostriction in two-dimensional antiferromagnets. *Nat. Mater.* **19**, 1295–1299 (2020).
7. Li, T. et al. Pressure-controlled interlayer magnetism in atomically thin CrI₃. *Nat. Mater.* **18**, 1303–1308 (2019).
8. Song, T. et al. Switching 2D magnetic states via pressure tuning of layer stacking. *Nat. Mater.* **18**, 1298–1302 (2019).
9. Tang, C., Zhang, L., Sanvito, S. & Du, A. Electric-controlled half-metallicity in magnetic van der Waals heterobilayer. *J. Mater. Chem. C* **8**, 7034–7040 (2020).
10. Bhoi, D. et al. Nearly room-temperature ferromagnetism in a pressure-induced correlated metallic state of the van der Waals insulator CrGeTe₃. *Phys. Rev. Lett.* **127**, 217203 (2021).
11. Li, Q. et al. Patterning-induced ferromagnetism of Fe₃GeTe₂ van der Waals materials beyond room temperature. *Nano Lett.* **18**, 5974–5980 (2018).
12. Vedmedenko, E. Y. et al. The 2020 magnetism roadmap. *J. Phys. D Appl. Phys.* **53**, 453001 (2020).
13. Stanciu, C. et al. All-optical magnetic recording with circularly polarized light. *Phys. Rev. Lett.* **99**, 047601 (2007).
14. Lambert, C.-H. et al. All-optical control of ferromagnetic thin films and nanostructures. *Science* **345**, 1337–1340 (2014).
15. Mangin, S. et al. Engineered materials for all-optical helicity-dependent magnetic switching. *Nat. Mater.* **13**, 286–292 (2014).
16. Chen, X.-J. Fundamental mechanism for all-optical helicity-dependent switching of magnetization. *Sci. Rep.* **7**, 41294 (2017).
17. El Hadri, M. S. et al. Two types of all-optical magnetization switching mechanisms using femtosecond laser pulses. *Phys. Rev. B* **94**, 064412 (2016).
18. van der Ziel, J. P., Pershan, P. S. & Malmstrom, L. D. Optically-induced magnetization resulting from the inverse Faraday effect. *Phys. Rev. Lett.* **15**, 190–193 (1965).
19. Zhang, H.-L., Wang, Y.-Z. & Chen, X.-J. A simple explanation for the inverse Faraday effect in metals. *J. Magn. Magn. Mater.* **321**, L73–L74 (2009).
20. Gorchon, J., Yang, Y. & Bokor, J. Model for multishot all-thermal all-optical switching in ferromagnets. *Phys. Rev. B* **94**, 020409 (2016).
21. Fernández-Rossier, J., Núñez, A. S., Abolfath, M. & MacDonald, A. Optical spin transfer in ferromagnetic semiconductors. Preprint at *arXiv* <https://doi.org/10.48550/arXiv.cond-mat/0304492> (2003).
22. Kudlis, A., Iorsh, I. & Shelykh, I. A. All-optical resonant magnetization switching in CrI₃ monolayers. *Phys. Rev. B* **104**, L020412 (2021).
23. Oiwa, A., Mitsumori, Y., Moriya, R., Slupinski, T. & Munekata, H. Effect of optical spin injection on ferromagnetically coupled Mn spins in the III-V magnetic alloy semiconductor (Ga,Mn)As. *Phys. Rev. Lett.* **88**, 137202 (2002).
24. Seyler, K. L. et al. Ligand-field helical luminescence in a 2D ferromagnetic insulator. *Nat. Phys.* **14**, 277–281 (2018).
25. Wu, M., Li, Z., Cao, T. & Louie, S. G. Physical origin of giant excitonic and magneto-optical responses in two-dimensional ferromagnetic insulators. *Nat. Commun.* **10**, 2371 (2019).
26. Hubert, A. & Schäfer, R. *Magnetic Domains: the Analysis of Magnetic Microstructures* (Springer Science & Business Media, 2008).
27. Khorsand, A. et al. Role of magnetic circular dichroism in all-optical magnetic recording. *Phys. Rev. Lett.* **108**, 127205 (2012).
28. Malitson, I. H. Refraction and dispersion of synthetic sapphire. *J. Opt. Soc. Am.* **52**, 1377–1379 (1962).
29. McIntyre, J. & Aspnes, D. E. Differential reflection spectroscopy of very thin surface films. *Surf. Sci.* **24**, 417–434 (1971).
30. Shcherbakov, D. et al. Raman spectroscopy, photocatalytic degradation, and stabilization of atomically thin chromium tri-iodide. *Nano Lett.* **18**, 4214–4219 (2018).
31. Cornelissen, T. D., Córdoba, R. & Koopmans, B. Microscopic model for all-optical switching in ferromagnets. *Appl. Phys. Lett.* **108**, 142405 (2016).
32. Molina-Sánchez, A., Catarina, G., Sangalli, D. & Fernandez-Rossier, J. Magneto-optical response of chromium trihalide monolayers: chemical trends. *J. Mater. Chem. C* **8**, 8856–8863 (2020).

Publisher's note Springer Nature remains neutral with regard to jurisdictional claims in published maps and institutional affiliations.

Springer Nature or its licensor holds exclusive rights to this article under a publishing agreement with the author(s) or other rightsholder(s); author self-archiving of the accepted manuscript version of this article is solely governed by the terms of such publishing agreement and applicable law.

© The Author(s), under exclusive licence to Springer Nature Limited 2022

Methods

Growth of CrI₃ bulk crystals. Bulk CrI₃ crystals were synthesized by chemical vapour transport, as described previously³⁰. The elements were sealed in an evacuated ampoule (109.0 mg Cr chunks, 1 equiv., Alfa Aesar, 99.999% purity; 798.0 mg I₂ crystals, 1.5 equiv, Alfa Aesar, 99.999% purity). The ampoule was heated to 650 °C at the feed and 550 °C at the growth zone. After a week, the ampoule was cooled, and the reaction yielded crystals with 1–2 mm edge length. CrI₃ produced by this method crystallized in the C2/m space group with typical lattice parameters of $a = 6.904 \text{ \AA}$, $b = 11.899 \text{ \AA}$, $c = 7.008 \text{ \AA}$ and $\beta = 108.74^\circ$ at room temperature. In a typical sample, the crystals exhibit a Curie temperature of 61 K as well as a structural phase transition to the space group R3 at 210–220 K (ref. ³³).

Sample preparation. Bulk CrI₃ crystals were exfoliated onto 300 nm SiO₂/Si substrates. Using the optical contrast between the flakes and the substrate, thin-layer flakes of CrI₃ were identified and either encapsulated with 40- to 50-nm-thick hBN flakes or picked up and transferred to sapphire substrates for all-optical magnetization switching or white light absorption measurements, respectively. The van der Waals assembly was created through a dry transfer technique with a stamp consisting of a poly(propylene) carbonate film stretched over a polydimethylsiloxane stack³⁴. To prevent CrI₃ samples from degradation, all steps of the assembly process were performed in a glove box with a N₂ atmosphere (<0.1 ppm of water and oxygen); all the optical measurements were carried out in either an attoDRY cryostat or a Montana cryostat in which the sample is kept under ultrahigh pure He gas or vacuum condition; and the samples were carried using a container filled with N₂ or He gas during transportation between the glove box and optical cryostat. The samples were exposed to air during the sample loading and unloading process for less than one minute. Under these conditions, we were able to study the same sample for magnetic switching behaviour for a total of nine sets of measurements in a period of ten months. In total, we studied the all-optical switching of magnetization on three CrI₃ samples (two hBN-encapsulated 3L CrI₃ samples (Supplementary Fig. 6) and one hBN-capped 5L CrI₃ on sapphire sample (Supplementary Fig. 7)). All showed similar magnetization switching behaviours.

Optical measurements. RMCD measurements of the CrI₃ samples were performed in an attoDRY 2100 cryostat with a base temperature of 1.6 K and an application of magnetic fields of up to 9 T. RMCD imaging, which is used to determine the magnetization state before and after the pulse laser excitation of the CrI₃ flakes, was acquired using a 632.8 nm He–Ne laser with a beam spot of ~1 μm in diameter and a power of ~5 μW. A magnetic-field-dependent RMCD hysteresis study was carried out using three continuous wave lasers with different wavelengths: 532 nm, 632.8 nm and 785 nm.

For the magnetization switching experiments (performed at 1.6 K), we used ultrafast laser pulses, with a central wavelength ranging from 525 to 860 nm, a pulse duration of ~100 fs, a repetition rate of 80 MHz and a beam spot of ~1.5 μm in diameter. The helicity of the light was controlled using a combination of a linear polarizer and a quarter-wave plate, which transforms linearly polarized light to either left (σ_+) or right (σ_-) circular polarization. To sweep the laser on the sample, a raster-scanning approach was used. The sample was placed on a piezoelectric scanner and was scanned with an average speed of ~0.6 μm s⁻¹. For a sample dimension of 15 μm by 10 μm (discussed in Figs. 1–3), it takes approximately 6 minutes (a total of 15 steps in the vertical direction) to complete a single scan. We used laser powers ranging from 0.5 to 13 mW to determine the switching fluence threshold.

For the white light reflectance measurements, the CrI₃/sapphire sample was mounted on a Montana cryostat with a base temperature of 4 K. A tungsten-halogen lamp was used as the white light source, and the reflected signal was detected using a Horiba spectrometer and an ultraviolet-enhanced Si CCD (charge-coupled device). The differential reflectance, $(R - R_0)/R_0$, was obtained by subtracting and normalizing the CrI₃ reflectance (R) by the reflectance of the bare sapphire substrate (R_0).

Data availability

The data that support the findings of this study are available from the corresponding author upon reasonable request.

References

33. McGuire, M. A., Dixit, H., Cooper, V. R. & Sales, B. C. Coupling of crystal structure and magnetism in the layered, ferromagnetic insulator CrI₃. *Chem. Mater.* **27**, 612–620 (2015).
34. Pizzocchero, F. et al. The hot pick-up technique for batch assembly of van der Waals heterostructures. *Nat. Commun.* **7**, 11894 (2016).

Acknowledgements

This work was primarily supported by the Gordon and Betty Moore Foundation (award no. 5722) and the Ernest S. Kuh Endowed Chair Professorship (P.Z., T.-F.C., Q.L., S.W., S.Y. and X.Z.). P.Z. thanks M. Wu and C. Hu for discussions. W.L.B.H. and J.E.G. acknowledge support from the Center for Emergent Materials, a National Science Foundation Materials Research Science and Engineering Center, under award number DMR-2011876. Q.W. and J.Y. acknowledge support from Intel Corporation under an award titled Valleytronics Center and US Department of Energy, Office of Science, Office of Basic Energy Sciences, Materials Sciences and Engineering Division under contract no. DE-AC02-05-CH11231 within the Organic-Inorganic Nano-composites Program (KC3104).

Author contributions

P.Z. and X.Z. initiated the project and designed the experiments. P.Z. prepared the samples with the assistance of T.-F.C.; P.Z. developed the all-optical magnetization switching set-up and performed all the optical measurements with the assistance of Q.L. and Q.W.; W.L.B.H. and J.E.G. grew the bulk CrI₃ crystals. T.-F.C., S.W. and S.Y. provided valuable insight and suggestions. X.Z. supervised the research. P.Z. analysed the data and wrote the manuscript. All the authors discussed the results and commented on the manuscript.

Competing interests

The authors declare no competing interests.

Additional information

Supplementary information The online version contains supplementary material available at <https://doi.org/10.1038/s41563-022-01354-7>.

Correspondence and requests for materials should be addressed to Xiang Zhang.

Peer review information *Nature Materials* thanks the anonymous reviewers for their contribution to the peer review of this work.

Reprints and permissions information is available at www.nature.com/reprints.